

TECHNICAL REPORT

Open Access



# A two-stage deflection system for the extension of the energy coverage in space plasma three-dimensional measurements

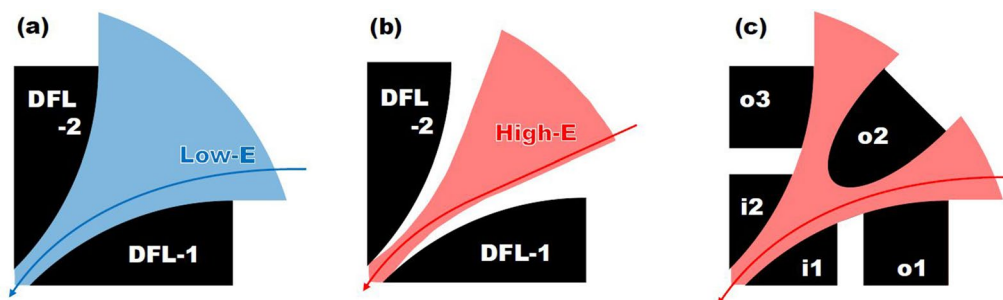
Satoshi Kasahara<sup>1\*</sup> , Ryo Tao<sup>1</sup>, Emiko Yoshida<sup>1</sup> and Shoichiro Yokota<sup>2</sup>

## Abstract

The in situ measurement of charged particles plays a key role in understanding space plasma physics. Velocity distribution functions of ions and electrons have been acquired with electrostatic analyzers onboard spacecraft. Since conventional energy analyzers (e.g., top-hat electrostatic analyzers) have essentially a two-dimensional field of view, the solid angle coverage is achieved with the aid of spacecraft spin motion or with additional entrance deflection systems in front of the electrostatic analyzer. In the latter case, however, the full angular scan is realized only in the lower energy range (typically only up to 5–15 keV/e), due to the limitation of the electric field applied to the deflector. Here we propose a novel deflection system for extending the energy coverage up to tens of keV. This is especially useful for plasma observations in situations where the anisotropy of the energetic part (> 10 keV) of charged particles plays an essential role in plasma dynamics and hence is of significant interest.

**Keywords** Deflector system, Electrostatic analyzer, In situ space plasma measurements

## Graphical Abstract



\*Correspondence:

Satoshi Kasahara  
s.kasahara@eps.s.u-tokyo.ac.jp

<sup>1</sup> Department of Earth and Planetary Science, Graduate School of Science, The University of Tokyo, Tokyo, Japan

<sup>2</sup> Graduate School of Science, Osaka University, Toyonaka, Japan



© The Author(s) 2023. **Open Access** This article is licensed under a Creative Commons Attribution 4.0 International License, which permits use, sharing, adaptation, distribution and reproduction in any medium or format, as long as you give appropriate credit to the original author(s) and the source, provide a link to the Creative Commons licence, and indicate if changes were made. The images or other third party material in this article are included in the article's Creative Commons licence, unless indicated otherwise in a credit line to the material. If material is not included in the article's Creative Commons licence and your intended use is not permitted by statutory regulation or exceeds the permitted use, you will need to obtain permission directly from the copyright holder. To view a copy of this licence, visit <http://creativecommons.org/licenses/by/4.0/>.

## Introduction

Direct measurement of plasma particles is a fundamental approach in studying space and planetary science. Acquisition of three-dimensional velocity distribution functions has been widely made using electrostatic analyzers (ESAs), by which the energy per charge and direction of each incoming charged particle can be identified (e.g., Carlson and McFadden 1998). Since conventional ESAs (e.g., top-hat electrostatic analyzers, see Carlson et al. 1983, Young et al. 1988) have a disk-shaped, essentially two-dimensional field of view, an additional mechanism is required for covering a broad solid angle. The coverage is demanded to be as close to as  $4\pi$  steradian, although often compromised at narrower values. One of the conventional methods to obtain a wide solid angle coverage is to utilize a motion of a platform (e.g., spacecraft spin and actuator platform). On the other hand, a deflector (DFL) system is a typical solution on a three-axis-stabilized spacecraft (Carlson and McFadden 1998; Yokota et al. 2005; Young et al. 2007; McFadden et al. 2015; Desai et al. 2016; McComas et al. 2017). A pair of electrodes (Fig. 1a) electrostatically deflect incoming particles before they enter an ESA. By sweeping the applied voltages on the electrodes, the elevation angle of the particles' incoming direction is scanned. The  $2\pi$  steradian field of view can be covered in combination with the ESA's azimuthal field of view. Such deflectors typically offer  $\sim 90^\circ$  angular coverage (Fig. 1a), but only for the limited energy range (typically up to 5–15 keV/e). The angular coverage becomes narrower for the higher energy range (Fig. 1b) unless the electric field applied to the gap between DFL electrodes is much higher than those applied to the gap between ESA electrodes. Since the higher electric field needs excessive requirements/resources on the high-voltage power supply and/or leads to the risk of discharging, the angular coverage in the higher energy range has been compromised in most previous applications.

The goal of this work is to achieve better angular coverage for a higher energy range ( $> 15$  keV/e) without

introducing a higher voltage for DFL than those for ESA. The broader angular coverage is essential for space plasma measurements in general, and specifically in the situation where the anisotropy provides important clues for revealing plasma structures (e.g., where the finite Larmor radius effect is observed) or analyzing wave-particle interaction.

## Concept and design

To realize the broader angular coverage for the higher energy, here we introduce the two-stage DFL system (Fig. 1c). In addition to a conventional pair of deflection plates (“i1” and “i2”), another set of deflectors (“o1”, “o2”, and “o3” in) are implemented. Under the voltage limitation, this concept essentially doubles the deflection capability, raising the uppermost energy for the  $\sim 90^\circ$  coverage. On the other hand, the size is not necessarily doubled as also schematically shown in Fig. 1.

The detailed structure based on this concept is shown in Fig. 2. The entrance DFL system, which is the main subject of this paper, is shown in the upper half (higher than 90 mm along the vertical axis). The lower half is a cusp-type ESA for energy measurements (Kasahara et al. 2006, 2018; Yokota et al. 2017; Ogasawara et al. 2018), which has an advantage in the higher-energy coverage compared to conventional top-hat type ESA (Carlson et al. 1983, Young et al. 1988). At the exit of the ESA, particle trajectories are radially inward because it is necessary to introduce ions into a linear-electric field time-of-flight mass analyses unit (Möbius et al. 1990; Hamilton et al. 1990; McComas and Nordholt 1990; Yokota et al. 2005, 2021; Gilbert et al. 2010) attached below the ESA (the detailed design and performance of the mass spectrometer are beyond the scope of the paper).

Here we aimed at covering a hemispherical ( $-45^\circ \pm 45^\circ$  elevation angle) field of view like IMA (Yokota et al. 2005) onboard Kaguya, compared to torus-shaped ( $0^\circ \pm 45^\circ$  elevation angle) DFL systems (Carlson and McFadden 1998; Young et al. 2007; McFadden et al.

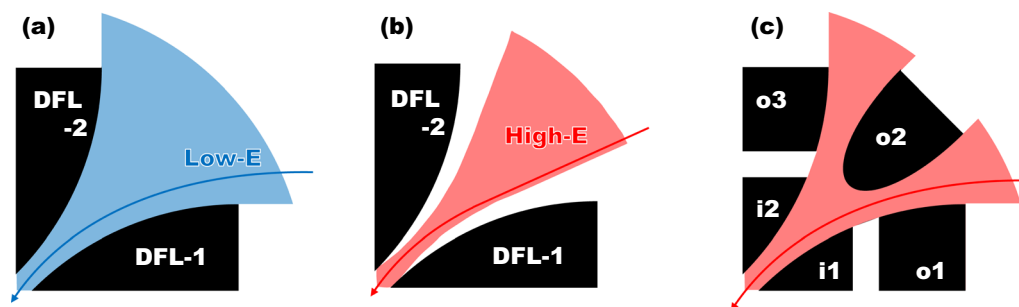


**Fig. 1** Schematic diagram illustrating the direction coverage of a conventional deflector for **a** low-energy and **b** high-energy, and **c** a two-staged deflector. The newly proposed deflector enables a broader coverage for higher energy without strengthening the electric field

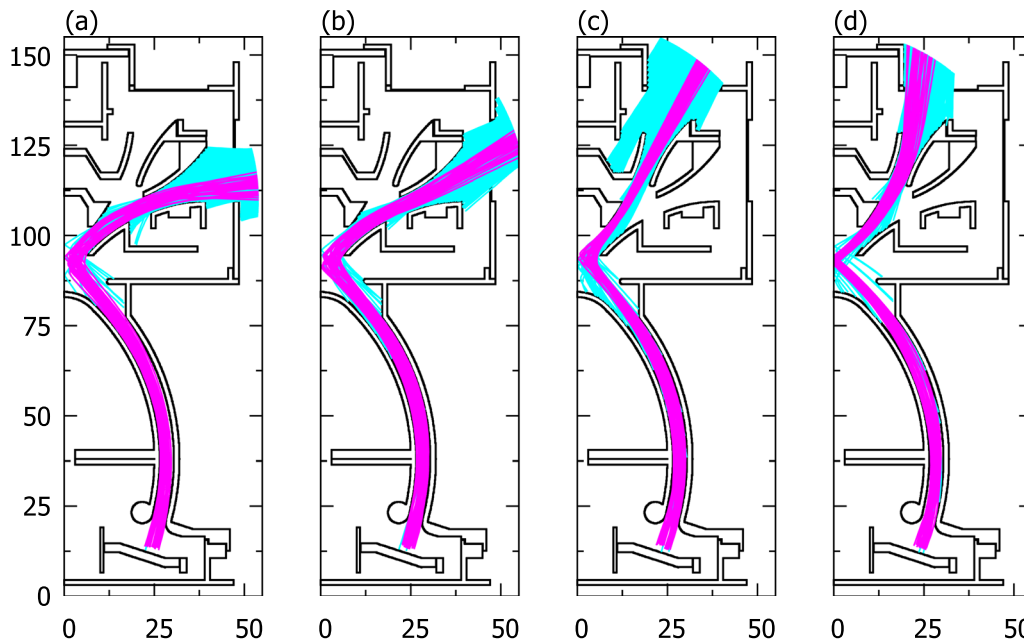


**Fig. 2** The electrode structures of the ion optics and four cases of particle trajectories (5 keV/e). The sensor’s symmetrical axis is at the left of each panel. Cases **a** “0°”, **b** “–30°”, **c** “–60°”, and **d** “–90°” are shown here. Ion trajectories passing through the deflector and the electrostatic analyzer are shown in magenta, while all the injected particles are in cyan. The number in the horizontal and vertical axes indicate dimensions in millimeter

2015; Desai et al. 2016; McComas et al. 2017). This choice is beneficial in the case that spacecraft structures below the sensor substantially interfere with the (lower hemisphere of the) field of view.

Most of the DFL electrodes have a curvature radius of 40 mm, while the radius of one of them (“i2”) was set to 50 mm after iterative simulations. The minimum gaps between electrodes are >4 mm so that the imposed electric field is <1.5 kV/mm (and typically ~1 kV/mm) at maximum with the maximum applied voltage of 5 kV. This maximum voltage (5 kV) is the same as that of ESA (but with the opposite polarity) since it is our prerequisite in this work. Note that the capability of the full angular coverage to higher energy is enhanced by the higher electric field. Nevertheless, we put the above threshold (1.5 kV/mm) for the DFL gap to avoid the risk of electric discharging and the decrease of the geometric factor. Here we use only positive deflection voltages to avoid producing beams of energetic photoelectrons, which could contaminate other measurements. Such photoelectrons may also lead to the failure of the high-voltage power supply.

By sweeping the set of applied voltages applied to the DFL electrodes (see Table 1), it can achieve ~90° coverage up to ~25 keV/e. Most importantly, the ratio  $V_{DFL}/V_{ESA}$  is less than 2, where  $V_{DFL}$  is the deflector voltage and  $V_{ESA}$  is the ESA voltage. This is compared to the typical value of ~4 for ±45° deflection in a conventional DFL system

**Table 1** Applied voltages for deflectors ( $V_{DFL}$ ) normalized by the voltage of the electrostatic analyzer ( $V_{ESA}$ )

	Case 1 (–0°)	Case 2 (–30°)	Case 3 (–60°)	Case 4 (–90°)
$-V_{DFL1}/V_{ESA}$	0	0	1.6	1.6
$-V_{DFL2}/V_{ESA}$	1.6	1.6	0	0
$-V_{DFL01}/V_{ESA}$	0	0.4	1.6	1.6
$-V_{DFL02}/V_{ESA}$	1.6	0	0	1.6
$-V_{DFL03}/V_{ESA}$	1.6	1.6	0	0

(Carlson and McFadden 1998). This indicates that the upper limit of our DFL energy coverage is doubled compared to the conventional DFL system. Figure 3 shows that the conventional trend is roughly evaluated by  $E_{MAX}(\text{keV/e}) = (1.5-2.5) \times V_{DFL\_MAX}$ , where  $E_{MAX}$  is the highest energy/charge of ±45° deflection and  $V_{DFL\_MAX}$  is the upper limit of the voltage difference applied to the deflection electrodes. The uppermost energy of our DFL system is substantially higher than this trend.

**Verification**

We have fabricated the deflector system as well as the ESA, followed by a time-of-flight mass analyses unit (Gilbert et al. 2010; Yokota et al. 2021). An  $N_2^+$  ion beam is injected into our ion sensor set inside a vacuum chamber. The transmittance (acceptance) of ions was measured

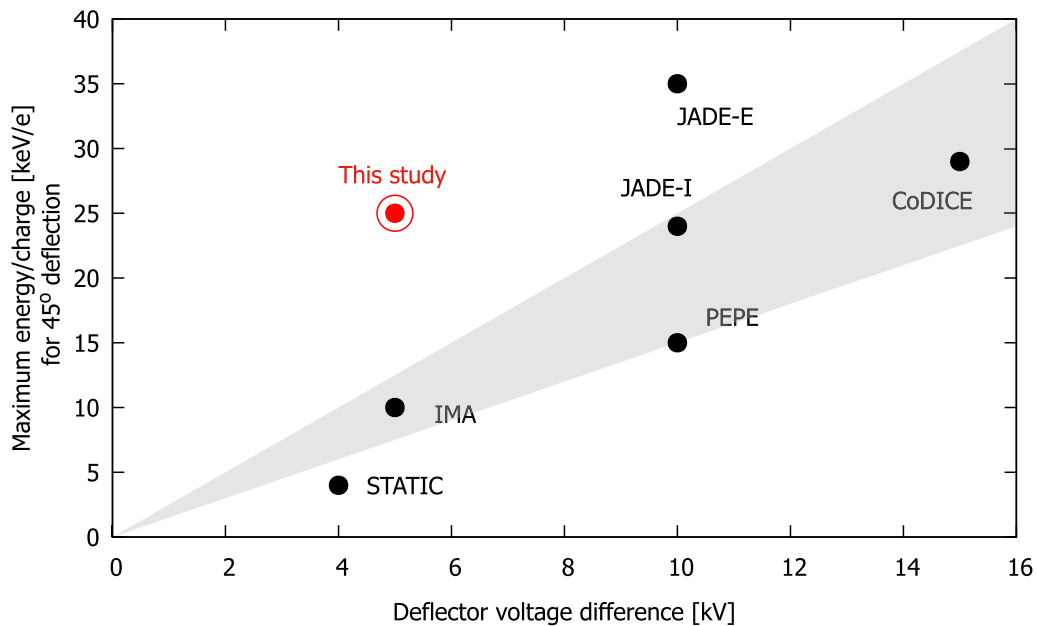


**Fig. 3** The relationship between the maximum energy-per-charge for  $\pm 45^\circ$  deflection and maximum deflector voltages of previous instruments (MAVEN/STATIC (McFadden et al. 2015), Deep Space I/PEPE (Young et al. 2007), JUNO/JADE-I and JADE-E (McComas et al. 2017), CoDICE (Desai et al. 2016), and Kaguya/IMA (Yokota et al. 2005)). The gray-shaded area indicates energy-voltage relationships  $E_{MAX}$  (keV/e) =  $2.5 V_{DFL\_MAX}$  (kV) (upper edge) and  $E_{MAX}$  (keV/e) =  $1.5 V_{DFL\_MAX}$  (kV) (lower edge), where  $E_{MAX}$  is the maximum energy/charge for  $45^\circ$  deflection and  $V_{DFL\_MAX}$  is the maximum deflector voltage difference. An exceptionally high  $E_{MAX}/V_{DFL\_MAX}$  ratio ( $\sim 3.5$ ) for JADE-E is realized by the strong electric field (see discussion in the main text)

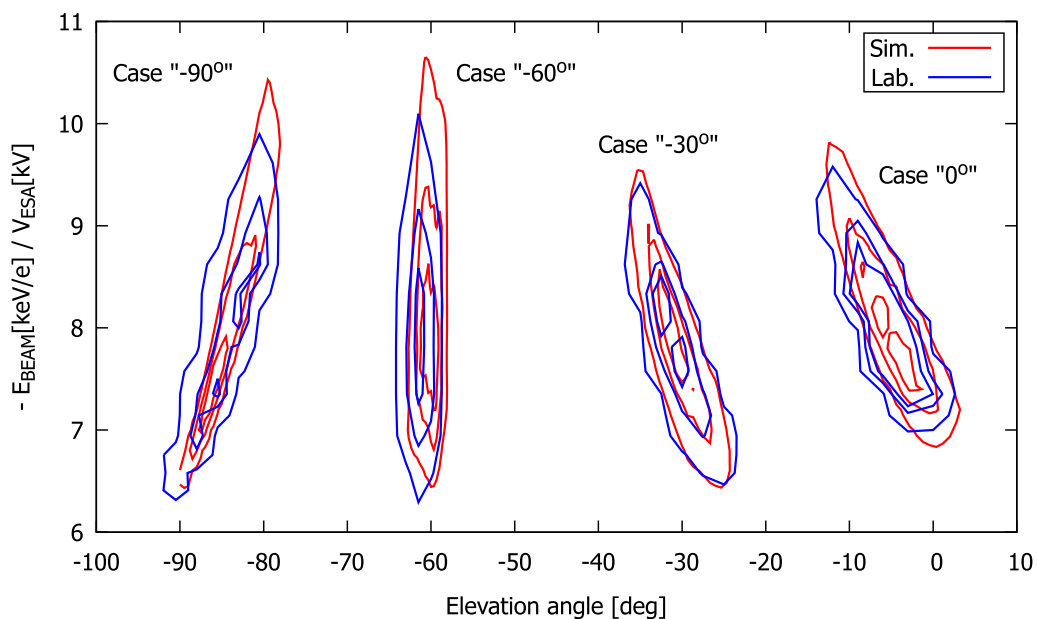


**Fig. 4** Transmittance as a function of the ion beam energy ( $E_{BEAM}$ ) and the elevation angle (red: simulation, blue: laboratory experiments). Contours are plotted for 10, 50, and 80% of the peak value. Four cases correspond to the trajectories in Fig. 3. The beam energy is normalized by the voltage of the electrostatic analyzer ( $V_{ESA}$ ). The deflector voltages ( $V_{DFL}$ ) are varied with a fixed  $V_{DFL}/V_{ESA}$  ratio following Table 1

and compared to numerical simulation results (Fig. 4). The beam energy/charge  $E_{\text{BEAM}}$  was fixed at 5 keV/e while  $V_{\text{ESA}}$  and  $V_{\text{DFL}}$  are varied. The ratio  $V_{\text{DFL}}/V_{\text{ESA}}$  was varied following Table 1. The incoming direction of the beam, referred to as the elevation angle, was varied by rotating the sensor with a gimbal system inside the vacuum chamber.

The test result is consistent with the simulation in terms of the center positions and widths in energy and angle, indicating that the sensor works as per the design. The elevation angle differences between the experiment and simulation are typically less than  $1^\circ$ , which is reasonably smaller than the angular resolution. The central energy  $E_{\text{BEAM}}/V_{\text{ESA}}$  is  $\sim 8$ , for which, again, the differences between the experiment and simulation are much smaller than the energy resolution (20–30%). This ratio ( $E_{\text{BEAM}}/V_{\text{ESA}} \sim 8$ ) is converted to  $E_{\text{BEAM}}/V_{\text{DFL}} \sim 5$  since  $V_{\text{DFL}}/V_{\text{ESA}}$  is  $\sim 1.6$  at maximum (Table 1). If we apply a moderate voltage of 5 kV (then the electric field is  $\sim 1$  kV/mm, which is moderate to avoid discharging), the uppermost energy for  $90^\circ$  coverage is 25 keV/e.

## Summary and discussion

In this paper, we designed the two-stage DFL system to double the energy coverage for acquiring three-dimensional plasma velocity distribution functions and fabricated a test model to verify the concept. The test result proved that the sensor works as per the design, achieving energy coverage up to 25 keV/e of the deflector system with the maximum applied voltage of 5 kV ( $E_{\text{BEAM}}/V_{\text{DFL}} \sim 5$ ). Note that the electric field is  $\sim 1$  kV/mm in our current design, which is moderate compared to 2 kV/mm or higher for other instruments (Young et al. 2007; McComas et al. 2017). For example, JADE-E onboard the JUNO spacecraft has an exceptionally high  $E_{\text{BEAM}}/V_{\text{DFL}}$  ( $\sim 3.5$ ) for a single-stage deflectors system (Fig. 3), which can be attributed to the strong electric field at the deflector. Our design achieves a higher  $E_{\text{BEAM}}/V_{\text{DFL}}$  with a moderate electric field. Even higher energy coverage can be achieved if a stronger electric field is applied. However, it should be noted that the stronger electric field needs a narrower DFL gap resulting in a lower geometrical factor (sensitivity) and/or a higher voltage difference incorporating more resources and a higher risk of discharging.

The two-stage DFL system has another possible advantage in terms of sensor sensitivity. While a homogeneous sensitivity for  $2\pi$ -steradian would be preferred for most applications, there may be some cases in which different sensitivities for different looking angles are demanded (e.g., in the solar wind). While the DFL design in this paper does not introduce a substantial difference in sensitivity for different looking directions, it is possible to

deliberately vary the geometrical factors between angles “ $0^\circ$  to  $-45^\circ$ ” and “ $-45^\circ$  to  $-90^\circ$ ”.

In this paper, we illustrated the advantage of our DFL design for a hemispherical (“ $-45^\circ \pm 45^\circ$ ” elevation angle) field of view (Yokota et al. 2005; 2021). While the verification studies are conducted by ions, our design can also be applied to electron measurements. Similar energy-angle responses are obtained through simulations for the electron incidence. In the electron case, the DFL voltages are kept positive, while the ESA voltage is switched to positive.

Adoption of our two-stage DFL system, which doubles the energy range of the full angular scan, is upon the trade-off with the resource. The proposed DFL system needs additional electrodes and applied high voltages (Fig. 1). While it does not double the size, it requires 5 independent high-voltage outputs (5 sets of opt-couplers), compared to conventional DFL systems working with 2 high-voltage outputs (2 sets of opt-couplers). This results in additional power consumption and mass of the sensor unit. To mitigate this, a possible measure is to connect the DFL-o3 electrode to DFL-i2 to reduce the number of high-voltage output (note that the applied voltages for these electrodes are the same in Table 1), at the expense of finer control of the deflection.

Our deflection system, enabling the extension of the energy range of three-dimensional velocity distribution function measurements, will be useful for future solar system science missions especially when energetic ions ( $> 10$  keV) are the key target.

## Abbreviations

DFL	Deflector
ESA	Electrostatic analyser
$V_{\text{DFL}}$	Deflector voltages
$V_{\text{ESA}}$	Voltage of the electrostatic analyzer
$E_{\text{BEAM}}$	Ion beam energy
$E_{\text{MAX}}$	Highest energy of $\pm 45^\circ$ deflection
$V_{\text{DFL\_MAX}}$	Upper limit of the voltage difference applied to the deflection electrodes

## Acknowledgements

Reviewers are acknowledged for their comments and suggestions for improving the manuscript.

## Author contributions

SK conducted conceptualization and sensor design, led laboratory experiments, and wrote the manuscript. RT and EY significantly contributed to the laboratory experiments and data analyses. SY widely contributed to the conceptualization, sensor design, and writing the manuscript. All authors read and approved the final manuscript.

## Funding

This work was supported by MEXT/JSPS KAKENHI grant 21H04509 (Grant-in-Aid for Scientific Research (A)).

## Availability of data and materials

The data that support the findings of this study are available from the corresponding author upon reasonable request.

## Declarations

### Ethics approval and consent to participate

Not applicable.

### Consent for publication

Not applicable.

### Competing interests

The authors declare that they have no competing interests.

Received: 16 December 2022 Accepted: 12 May 2023

Published online: 25 May 2023

## References

- Carlson CW, McFadden JP (1998) Design and Application of Imaging Plasma Instruments. In: Pfaff RF, Borovsky J, Young DT (eds) *Measurement Techniques in Space Plasmas Particles*. American Geophysical Union, Washington
- Carlson CW, Curtis DW, Paschmann G, Michael W (1983) An instrument for rapidly measuring plasma distribution functions with high resolution. *Adv Space Res*. [https://doi.org/10.1016/0273-1177\(82\)90151-X](https://doi.org/10.1016/0273-1177(82)90151-X)
- Desai MI, Ogasawara K, Ebert RW, Allegrini F, McComas DJ, Livi S, Weidner SE (2016) Compact dual ion composition experiment for space plasmas — CoDICE. *J Geophys Res Space Phys*. <https://doi.org/10.1002/2016JA022387>
- Gilbert JA, Lundgren RA, Panning MH, Rogacki S, Zurbuchen TH (2010) An optimized three-dimensional linear-electric-field time-of-flight analyzer. *Rev Sci Instrum*. <https://doi.org/10.1063/1.3429941>
- Hamilton DC, Gloeckler G, Ipavich FM, Lundgren RA, Sheldon RB, Hovestadt D (1990) New high-resolution electrostatic ion mass analyzer using time of flight. *Rev Sci Instrum*. <https://doi.org/10.1063/1.1141695>
- Kasahara S, Asamura K, Saito Y, Takashima T, Hirahara M, Mukai T (2006) Cusp type electrostatic analyzer for measurements of medium energy charged particles. *Rev Sci Instrum*. <https://doi.org/10.1063/1.2405358>
- Kasahara S, Yokota S, Mitani T et al (2018) Medium-energy particle experiments—electron analyzer (MEP-e) for the exploration of energization and radiation in geospace (ERG) mission. *Earth Planets Space* 70:69. <https://doi.org/10.1186/s40623-018-0847-z>
- McComas DJ, Nordholt JE (1990) New approach to 3-D, high sensitivity, high mass resolution space plasma composition measurements. *Rev Sci Instrum*. <https://doi.org/10.1063/1.1141692>
- McComas DJ et al (2017) The Jovian Auroral Distributions Experiment (JADE) on the Juno Mission to Jupiter. *Space Sci Rev* 213:547–643. <https://doi.org/10.1007/s11214-013-9990-9>
- McFadden JP et al (2015) MAVEN suprathermal and thermal ion composition (STATIC) instrument. *Space Sci Rev*. <https://doi.org/10.1007/s11214-015-0175-6>
- Möbius E, Bochsler P, Ghielmetti AG, Hamilton DC (1990) High mass resolution isochronous time-of-flight spectrograph for three-dimensional space plasma measurements. *Rev Sci Instrum*. <https://doi.org/10.1063/1.1141580>
- Ogasawara K, Allegrini F, Desai MI, Ebert RW, Fuselier SA, Jahn J-M, Livi SA, McComas DJ (2018) A double-cusp type electrostatic analyzer for high-cadence solar-wind suprathermal ion observations. *Rev Sci Instrum* 89(11):114503. <https://doi.org/10.1063/1.5030123>
- Yokota S, Saito Y, Asamura K, Mukai T (2005) Development of an ion energy mass spectrometer for application on board three-axis stabilized spacecraft. *Rev Sci Instrum* 76:14501. <https://doi.org/10.1063/1.1834697>
- Yokota S, Kasahara S, Mitani T et al (2017) Medium-energy particle experiments—ion mass analyzer (MEP-i) onboard ERG (Arase). *Earth Planets Space* 69:172. <https://doi.org/10.1186/s40623-017-0754-8>
- Yokota S, Terada N, Matsuoka A et al (2021) In situ observations of ions and magnetic field around Phobos: the mass spectrum analyzer (MSA) for the Martian Moons eXploration (MMX) mission. *Earth Planets Space* 73:216. <https://doi.org/10.1186/s40623-021-01452-x>
- Young DT et al (1988) 2 $\pi$ -radian field-of-view toroidal electrostatic analyzer. *Rev Sci Instrum*. <https://doi.org/10.1063/1.1139821>
- Young DT, Nordholt JE, Burch JL et al (2007) Plasma experiment for planetary exploration (PEPE). *Space Sci Rev*. <https://doi.org/10.1007/s11214-007-9177-3>

## Publisher's Note

Springer Nature remains neutral with regard to jurisdictional claims in published maps and institutional affiliations.

Submit your manuscript to a SpringerOpen<sup>®</sup> journal and benefit from:

- Convenient online submission
- Rigorous peer review
- Open access: articles freely available online
- High visibility within the field
- Retaining the copyright to your article

Submit your next manuscript at ► [springeropen.com](https://www.springeropen.com)